Thieme

Dual-Energy Computed Tomography for Fat Quantification in the Liver and Bone Marrow: A Literature Review

Dual-Energy-Computertomografie zur Fettquantifizierung in der Leber und im Knochenmark – ein Literatur-Review

Authors
Isabel Molwitz, Miriam Leiderer, Cansu Özden, Jin Yamamura

Affiliation
Department of Diagnostic and Interventional Radiology and Nuclear Medicine, University Medical Center Hamburg-Eppendorf, Hamburg, Germany

Key words
CT-quantitative, bone marrow, bone densitometry, dual-energy CT, fat quantification, hepatic steatosis

received 10.04.2020
accepted 11.06.2020
published online 10.09.2020

Bibliography
Fortschr Röntgenstr 2020; 192: 1137–1152
DOI 10.1055/a-1212-6017
ISSN 1438-9029

Georg Thieme Verlag KG, Rüdigerstraße 14, 70469 Stuttgart, Germany

Correspondence
Isabel Molwitz
Department of Diagnostic and Interventional Radiology and Nuclear Medicine, University Medical Center Hamburg-Eppendorf, Martinistraße 52, 20246 Hamburg, Germany
Tel.: + 49/40/7 41 05 40 10
i.molwitz@uke.de

ABSTRACT

Background With dual-energy computed tomography (DECT) it is possible to quantify certain elements and tissues by their specific attenuation, which is dependent on the X-ray spectrum. This systematic review provides an overview of the suitability of DECT for fat quantification in clinical diagnostics compared to established methods, such as histology, magnetic resonance imaging (MRI) and single-energy computed tomography (SECT).

Method Following a systematic literature search, studies which validated DECT fat quantification by other modalities were included. The methodological heterogeneity of all included studies was processed. The study results are presented and discussed according to the target organ and specifically for each modality of comparison.

Results Heterogeneity of the study methodology was high. The DECT data was generated by sequential CT scans, fast-kVp-switching DECT, or dual-source DECT. All included studies focused on the suitability of DECT for the diagnosis of hepatic steatosis and for the determination of the bone marrow fat percentage and the influence of bone marrow fat on the measurement of bone mineral density. Fat quantification in the liver and bone marrow by DECT showed valid results compared to histology, MRI chemical shift relaxometry, magnetic resonance spectroscopy, and SECT. For determination of hepatic steatosis in contrast-enhanced CT images, DECT was clearly superior to SECT. The measurement of bone marrow fat percentage via DECT enabled the bone mineral density quantification more reliably.

Conclusion DECT is an overall valid method for fat quantification in the liver and bone marrow. In contrast to SECT, it is especially advantageous to diagnose hepatic steatosis in contrast-enhanced CT examinations. In the bone marrow DECT fat quantification allows more valid quantification of bone mineral density than conventional methods. Complementary studies concerning DECT fat quantification by split-filter DECT or dual-layer spectral CT and further studies on other organ systems should be conducted.

Key points:
- DECT fat quantification in the liver and bone marrow is reliable.
- DECT is clearly superior to SECT in contrast-enhanced CT images.
- DECT bone marrow fat quantification enables better bone mineral density determination.
- Complementary studies with split-filter DECT or dual-layer spectral CT as well as studies in other organ systems are recommended.

Citation Format
- Molwitz I, Leiderer M, Özden C et al. Dual-Energy Computed Tomography for Fat Quantification in the Liver and Bone Marrow: A Literature Review. Fortschr Röntgenstr 2020; 192: 1137–1152

ZUSAMMENFASSUNG

Hintergrund Mit der Dual-Energy-Computertomografie (DECT) ist es möglich, bestimmte Elemente und Gewebe durch ihre spezifische, vom Röntgenspektrum abhängige Abschwächung zu quantifizieren. Diese systematische Übersichtsarbeit bietet einen Überblick über den Einsatz der DECT zur Fettquantifizierung in der klinischen Diagnostik im Vergleich zu etablierten Verfahren wie der Histologie, Magnetresonanztomografie (MRT) oder Single-Energy-Computertomografie (SECT).

Methode Nach systematischer Literaturrecherche wurden sämtliche Studien eingeschlossen, in denen Fettquantifizierung durch die DECT anhand von Vergleichsmodalitäten validiert wurde. Es erfolgte die Aufarbeitung der methodischen Heterogenität der eingeschlossenen Studien. Die Studienergebnisse wurden je Zielorgan und separat nach Vergleichsmodalitäten präsentiert und eingeordnet.

Ergebnisse Es bestand eine hohe Heterogenität der Studienmethodik. Die DECT-Daten basierten auf sequenzieller Generierung, Fast-kVp-Switching-DECT oder Dual-Source-DECT. Die Studien behandelten sämtlich die Eignung der DECT zur Diagnostik der Steatosis hepatis oder zur Bestimmung des Knochenmarkfettanteils und dessen Einfluss auf die Messung der Knochenmineraldichte. Die DECT-Fettquantifizierung in Leber und Knochenmark kommt gegenüber der Histologie, MRT-Chemical-Shift-Relaxometrie, Magnetresonanzspektroskopie und SECT zu validen Ergebnissen. In kontrastmittelgestützten CT-Aufnahmen ist die DECT der SECT zur Diagnostik der Steatosis hepatis klar überlegen. Im Knochen ermöglicht die Bestimmung des Knochenmarkfettanteils über die DECT die zuverlässigere Bestimmung auch des Knochenmineralanteils.

Schlussfolgerung Die DECT ist eine valide Methode zur Fettquantifizierung in Leber und Knochenmark und insbesondere für die Diagnostik der Steatosis hepatis in kontrastmittelgestützten CT-Untersuchungen gegenüber der SECT vorteilhaft. Die Korrektur der Knochenmineraldichte um den durch die DECT bestimmten Knochenmarkfettanteil gestattet eine exaktere Bestimmung der Knochenmineraldichte als konventionelle Methoden. Bei heterogener sowie fehlender Studienlage zur Split-Filter-DECT oder Dual-Layer-Spektral-CT besteht Bedarf an ergänzenden Arbeiten wie auch Potenzial für weitere Studien zur DECT-Fettquantifizierung in anderen Organsystemen.

Introduction

Reliable fat quantification is medically important for the diagnosis of hepatic steatosis in non-alcoholic fatty liver disease. The latter is a risk factor for the development of hepatocellular carcinoma [1].

Fat quantification is also relevant in bone since an inverse relationship between bone marrow fat and bone mineral density has been described [2]. High bone marrow fat percentages additionally distort the results of bone mineral density measurements [3] used to detect osteoporosis for the purpose of fracture prevention. An increased bone marrow fat percentage was also documented as an independent risk factor for fractures [2]. Fat quantification can also be used to differentiate benign from malignant lesions as in adrenal masses [4].

Fat quantification can be performed with the help of various imaging modalities, such as chemical shift relaxometry in magnetic resonance imaging (MRI) or magnetic resonance spectroscopy (MRS). Both methods provide objective quantitative values with MRS being considered the reference standard [5]. The measurement area of only a few cubic centimeter is a limitation in MRS. As a result, multiple time-intensive measurements are needed to cover entire organs or to detect irregular fatty lesions. In ultrasound, clinical fat measurement is typically performed in a qualitative manner by subjectively assessing the echogenicity compared to reference tissues [6]. However, there are also quantitative fat measurement approaches in ultrasound, including the use of backscatter coefficients or controlled attenuation parameters (FibroScan, Echosens, France) [6]. It is a disadvantage that calculation using backscatter coefficients requires reference phantoms and FibroScan shows some measurement errors in overweight female patients [6]. In single-energy computed tomography (SECT), semiquantitative fat measurement can be performed using attenuation coefficients in Hounsfield units (HU). However, since the attenuation coefficients are affected by the CT parameters and all materials within a voxel, both the reliability and the validity of measurements after contrast agent administration or in the case of iron deposits are limited [7].

A fat quantification method that has become increasingly available in recent years is dual-energy computed tomography (DECT). While the fundamental principle of DECT was described already in the early days of CT imaging [8, 9], the devices introduced in 2006 first made it possible to generate dual-energy data that is valid for clinical diagnosis in a single scan.

The goal of this review is to provide a critical evaluation and assessment of DECT fat quantification compared to established methods, i. e., histology, MRI, MRS, and SECT.

Technical background

In DECT, element/material-specific energy-dependent attenuation coefficients can be used to differentiate elements with different atomic numbers from one another [10]. It is also possible to quantify fat compared to other body tissues in this manner. The various energy spectra that are needed can be generated by sequential scans with a high and low tube voltage [11], by two separate tube detector systems (dual-source DECT) [12], or with an X-ray tube that switches in milliseconds between high and low voltage (fast-kVp-switching DECT) [11]. Moreover, split filters made of two different materials like tin and gold can be used at the tube output to generate high- and low-energy spectra [13, 14]. Separating the spectra on the detector level by means of layers of different materials superimposed over one another that absorb high-energy or low-energy photons is a further option (dual-layer spectral CT) [15]. All of these DECT techniques are shown as examples in ▶ **Fig. 1**.

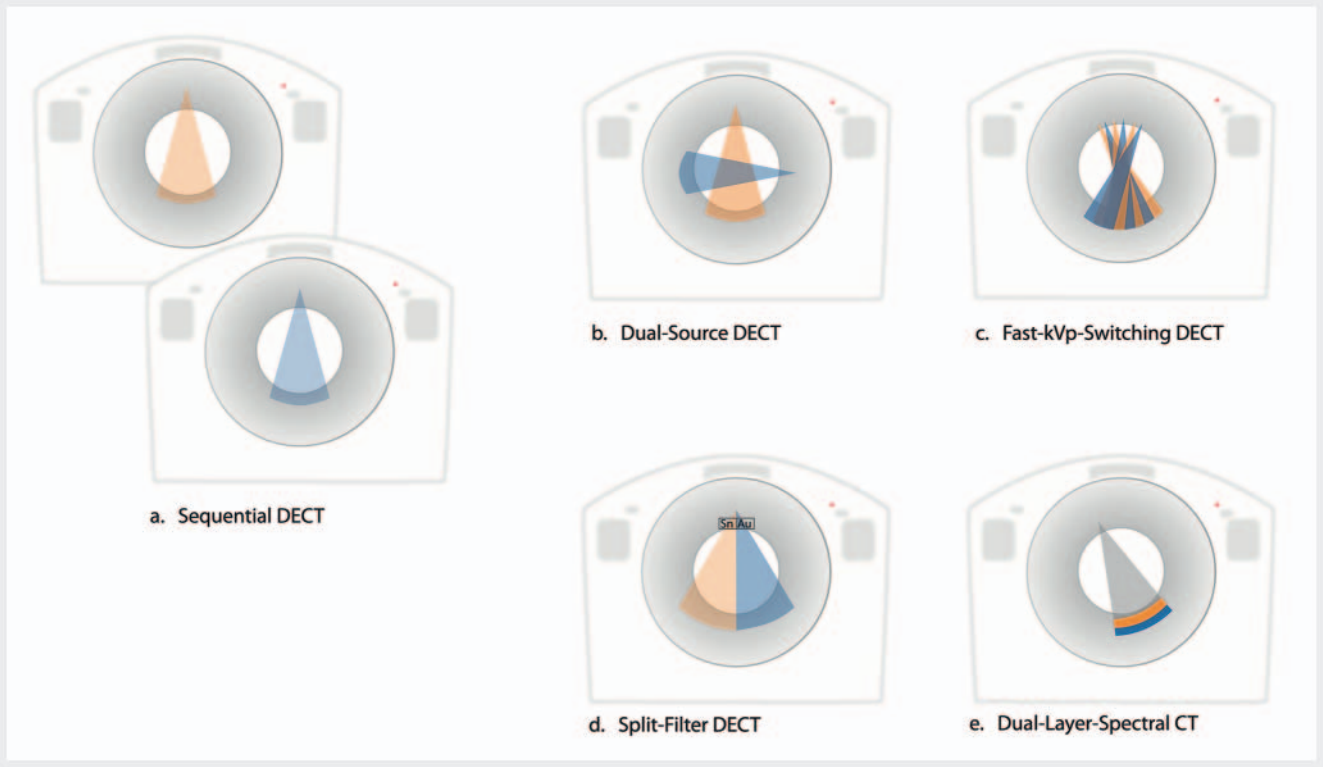

▶ **Fig. 1** Overview of the different scanner types that are capable of generating dual-energy data. The different options to generate dual-energy data are displayed. In sequential Dual-Energy CT (DECT) (a.) scans with high and low tube voltage are carried out one after the other. To generate high and low energy spectra without any time lapse Dual-Source CT (b.) which consists of two separate tube detector systems can be used. Switching between both energy levels within milliseconds is the approach of Fast-kVp-Switching CT (c.). Low-energy and high-energy spectra can also be generated by a split filter of two different materials like tin and gold which is placed at the tube output (d.). Separation of the spectra at the detector level by layers of different materials, as in Dual-Layer Spectral CT, is also possible (e.).

Method

The literature search with used search parameters, search parameters, and the approach used for study selection are shown in ▶ **Fig. 2**. The initial search of the medical database PubMed on 10/1/2019 yielded 61 hits. Original studies in which DECT fat quantification was compared to the measurement results of histology, MRI, or SECT were included. Studies in which the fat content was calculated by DECT but was not validated by comparison modalities were excluded. Moreover, phantom studies without ex or in vivo validation in animals or humans, conference proceedings, and studies without a full text in English or German were also excluded. Eight studies were selected based on the inclusion and exclusion criteria. Two reviews regarding fat imaging in the liver and bone marrow were also identified [16, 17]. One additional study for inclusion was identified by a Google search. The lists of references of all included studies and the two reviews were screened. This yielded ten additional studies. In total, 19 studies, 14 on DECT fat quantification in the liver and 5 on DECT fat quantification in bone marrow, were included. Concerning other organ systems one study examining the differentiation of adrenal metastases from adrenal adenomas via DECT fat quantification based on material decomposition showed a significantly lower fat concentration in the metastases [4]. However, there was no comparison modality like histology, MRI, or SECT to confirm the calculated fat percentage [4]. In accordance with the defined inclusion and exclusion criteria, this study was not included. All studies on other organ systems from the literature search addressed fat detection and not fat quantification and were accordingly also excluded. For example, DECT fat detection was used in these studies for differentiating surgically confirmed cholesterol gallstones from bile [18], for differentiating ex vivo myocardial muscle or thrombi from fat [19], for determining the ideal keV values for detecting coronary plaque containing fat or calcium [20], and for detecting pulmonary fat embolisms in rabbits [21].

Tables 1, 2 provide a comparison of the study design and methodology of all included studies.

The definition of SECT analyses compared to DECT analyses varied between the studies. For the sake of standardization, all analyses of attenuation coefficients (HU) on non-virtually generated images at any kV value are considered SECT results in the following. Analyses that can only be generated based on DECT scans are considered DECT results. This relates to virtual monoenergetic images used to define or determine, for example, attenuation coefficients in the liver or spleen. The HU differences between images at different k(e)V settings referred to in the following as DECT-ΔHU, e. g. the HU value at 140 k(e)V minus the HU value at 80 k(e)V, are also considered DECT results. Further DECT results are the effective Z-values recorded in two studies and the fat

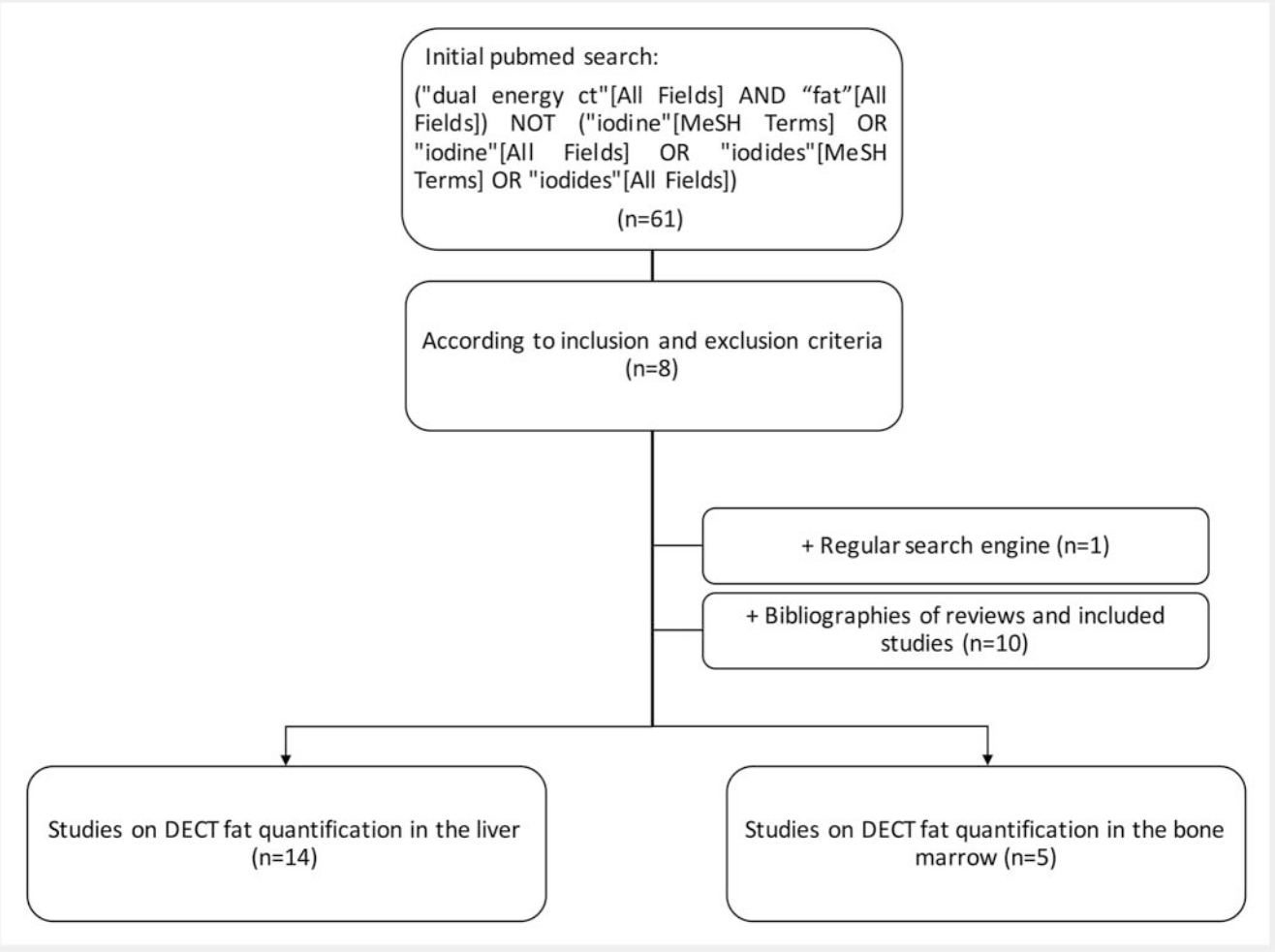

▶ **Fig. 2** Flowchart of search algorithm. The initial search in the medical database PubMed resulted in 61 results on October 1, 2019. Original papers that compared dual-energy CT fat quantification to established techniques (histology, MRI, single-energy CT) were included. Exclusion criteria were studies in which the measured fat content was not validated specifically, phantom studies without in vivo validation, conference proceedings and studies without full texts in English or German. This resulted in eight studies and two reviews about fat quantification in the liver and bone marrow. A supplementary search using a common search engine (Google) led to one additional primary source. Based on the literature of all included studies and both reviews, 10 further original articles were identified. Ultimately, 19 studies were included, 14 of them concerning fat quantification in the liver and 5 relating to fat quantification in bone marrow.

fraction calculated in the majority of the studies (n = 14) based on material decomposition (DECT-FF).

Results: Fat quantification in the liver

Among the 14 studies on fat quantification in the liver, DECT fat quantification was compared to histology in 9 studies [22–30], to MRI chemical shift relaxometry in 5 studies [5, 24, 25, 27, 28], to MRS in 4 studies [5, 25, 28, 29], and to SECT in 9 studies [5, 22, 24, 27, 28, 31–34] (see ▶ **Table 1**). An overview of the results of each study is shown in ▶ **Table 3**.

Value of DECT compared to histology

In the studies in which DECT was compared to histology, the DECT data in the oldest studies (1998 and 2003) was generated sequentially [22, 23]. DECT data was then collected with fast-kVP-switching DECT [24, 25, 27, 29, 30] and, starting in 2014, also sometimes with dual-source DECT [26, 28]. Only two studies examined patients (primarily steatosis on ultrasound) [22, 29]. The remaining measurements were performed in rats and rabbits.

DECT results were correlated to the histological grade of hepatic steatosis. A differentiation is made between mild fatty liver with a fat percentage of 0–33 %, moderate with a fat percentage of 33–66 %, and severe hepatic steatosis with a fat percentage of > 66 % [35]. In the majority of studies, DECT analyses correlated well with this histological classification.

The greatest correlation was seen for DECT-ΔHU in a sequential DECT study in rabbits (r = 0.95, for 90, 120 kV [23]). Assuming that this study result is valid, the level of correlation corresponds to that of histology with MRS, which is considered the gold standard of radiological fat quantification (r = 0.916 [28], r = 0.894 [25]). An also good but slightly smaller correlation with histology was indicated for attenuation coefficients on virtual monoenergetic ima-

▶ **Table 1** Overview of included studies concerning liver fat quantification by DECT.

Title	Author	Year	Study design	Number	Study object	Modality of comparison	DECT parameters	Scanner type
Dual-energy CT in the diagnosis and quantification of fatty liver: limited clinical value in comparison to ultrasound scan and single-energy CT, with special reference to iron overload	Mendler MH et al.	1998	Controlled cohort study	16 steatosis patients (11 with iron overload and 5 without), 11 control subjects	Patients	In the case of ultrasound-suspected steatosis: histology (fat vacuoles per number of hepatocytes), in any case: laboratory (i. e. CRP, TGL, cholesterol, glucose, serum iron, transferrin saturation, ferritin, ASAT, ALAT, GGT, AP, bilirubin, prothrombin time, factor V), SECT (native and post-contrast agent, 140 kV/130 mA, 10 mm slice thickness, HU values left and right hepatic, spleen (n = 21), paraspinal muscles, aorta and subcutaneous fat), liver ultrasound (4 degrees based on echogenicity)	Native, 80 kV/130 mA, 140 kV/130 mA, 10 mm slice thickness, HU values and DECT-ΔHU between 80 kV and 140 kV in identical measurement regions as for SECT analyses	GE CT Pace-Plus (sequential, General Electric)
Quantitative diagnosis of fatty liver with dual-energy CT: An experimental study in rabbits	Wang B et al.	2003	Randomized controlled trial	16 (fatty diet after 1, 2, 3 and 4 weeks), 4 controls	Rabbits	Histology (classification dependent on 33.3 %, 66.6 %, 100 % fat per field of view; fat percentage via automatic image analysis)	Native, 90 kV/150 mAs, 120 kV/100 mAs, collimation and slice thickness 5 mm, pitch 1 mm, HU values at 90 and 120 kV, DECT-ΔHU	HeliCAT flash (sequential, Elscint)
Quantification of hepatic steatosis with dual-energy computed tomography: comparison with tissue reference standards and quantitative magnetic resonance imaging in the ob/ob mouse	Artz NS et al.	2012	Controlled study	5 phantoms, 20 mice (6 × wild type, 7 × 4-week-old and 7 × 8-week-old leptin deficient ob/ob mouse)	Phantoms (0 %, 10 %, 20 %, 30 %, 50 % fat), wild type mice, ob/ob mice	Histology (fat percentage < 5 %, 5–33 %, 33–66 %, > 66 %), triglyceride mass fraction, MRI-FF (IDEAL, TR 300 ms, 5 echoes per TR, 15 total echoes, FA 3°), SECT (native, 100 kV/100 mA)	Native, 80/140 kV, 630 mA, slice thickness 0.6 mm, HU at 65 keV, DECT-FF (mg/ml), effective Z	GE Discovery CT750 HD (Fast-kVp-Switching, General Electric) 3 T MR750 v22.0' (General Electric)
Assessment of hepatic fatty infiltration using spectral computed tomography imaging: A pilot study	Zheng X et al.	2013	Controlled study	5 phantoms, 26 steatosis patients (5 × mild, 11 × moderate, 10 × severe steatosis hepatis), 20 control subjects	Phantoms (15 %, 30 %, 40 %, 70 %, 100 % fat), patients, healthy subjects	Known phantom fat concentration, determination of patient groups based on previous imaging results (CT, ultrasound)	Abdominal protocol without information on contrast agent application, 80/140 kV, 600 mA, collimation 0.625, slice thickness for final analyses 2.5 mm, distance 5 mm, pitch 1.25, HU on virtual monoenergetic images at 40, 50, 60, 70, 75, 100, 120 and 140 keV, HU on subtraction images 75 keV–50 keV	GE Discovery CT750 HD

▶ **Table 1** (Continuation)

Title	Author	Year	Study design	Number	Study object	Modality of comparison	DECT parameters	Scanner type
Contrast-independent liver-fat quantification from spectral CT exams	Mendonça PRS et al.	2013	Cohort study	6 phantoms, 50 patients	Phantoms (0 %, 10 %, 20 %, 30 %, 50 %, 100 % fat), patients (steatosis to varying degrees)	Known phantom fat concentration, MRI-FF of the phantoms (IDEAL), native CT values in patients	Native and contrast-enhanced (50 × native, 13 × arterial, 50 × portal-venous, 40 × late phase), DECT-FF (%)	GE Discovery CT750 HD GE Discovery MR750 W (General Electric)
Material density hepatic steatosis quantification on intravenous contrast-enhanced rapid kilovolt (peak)-switching single-source dual-energy computed tomography	Patel BN et al.	2013	Controlled cohort study	107 steatosis patients, 229 control subjects	Steatosis patients (liver spleen difference in HU < 1), control subjects (liver spleen difference > 1)	Native and contrast-enhanced SECT-HU	Native and contrast-enhanced (arterial, portal-venous phase), collimation 0.625 mm, slice thickness 5 mm, pitch 1.375, DECT-FF (mg/ml)	GE Discovery CT750 HD
A Flexible Method for Multi-Material Decomposition of Dual-Energy CT Images	Mendonça PRS et al.	2014	Cohort study	Please see Mendonça PRS et al. 2013	Please see Mendonça PRS et al. 2013	Please see Mendonça PRS et al. 2013	Please see Mendonça PRS et al. 2013	Please see Mendonça PRS et al. 2013
Evaluation of hepatic steatosis using dual-energy CT with MR comparison	Sun T et al.	2014	Randomized controlled trial	41 (fatty diet), 10 controls	Rats	Histology (< 5 %, 5–33 %, 33–66 %, > 66 %), MRI-FF (dual-phase, TR 150 ms, TE 1.4 ms, FA 75°), MRS (TR 2000 ms, TE 35 ms, 64 acquisitions)	Native, 80/140 kV, 630 mA, HU at 40 keV, effective Z, DECT-FF (mg/ml)	GE Discovery CT750 HD 3 T Signa MR (General Electric)
Separation of Hepatic Iron and Fat by Dual-Source Dual-Energy Computed Tomography Based on Material Decomposition: An Animal Study	Ma J et al.	2014	Controlled study	55 (9 × steatosis only, 9 × iron overload only, 37 × steatosis and iron overload), 5 controls	Rats	Histology (< 5 %, 5–33 %, > 33 %; for statistical analyses only classification results of less and more than 5 % were used)	Native, 80 kV/323 mA, Sn 140 kV/96 mA, collimation 0.6 mm, slice thickness 3 mm, increment 2 mm, pitch 0.6, HU values on virtual non-iron maps	SOMATOM Definition Flash (Siemens)
Quantification of the fat fraction in the liver using dual-energy computed tomography and multimaterial decomposition	Hur BY et al.	2014	Randomized controlled trial	12 (fatty diet: 4 × 2 weeks, 4 × 4 weeks, 4 × 6 weeks), 4 controls	Rabbits	Histology (< 5 %, 5–33 %, 33–66 %, > 66 %), MRI-FF (TR 16.2 ms, TE 1.8 ms, FA 8°, IDEAL), native SECT-HU (120 kV, 400 mA, slice thickness 5 mm, pitch 1)	20 s after contrast injection, 80/140 kV, 550 mA, slice thickness 5 mm, pitch 1, DECT-FF (%)	GE Discovery CT750 HD 1 T SignaHDxt (General Electric)

▶ **Table 1** (Continuation)

Title	Author	Year	Study design	Number	Study object	Modality of comparison	DECT parameters	Scanner type
Accuracy of Liver Fat Quantification With Advanced CT, MRI, and Ultrasound Techniques: Prospective Comparison With MR Spectroscopy	Kramer H et al.	2017		50	CT-colonography patients	SECT-HU (native 120 kV, 1.25 mm slice thickness), MRI-FF (TR 13.6 ms, first TE 1.2 mm, overall 6 echoes, FA 5°), MRS (TR 3500 ms, TE 10, 20, 30, 40 und 50 ms), ultrasound (4 degrees based on echogenicity), elastography	Native, 80/140 kV, virtual monoenergetic images at 70, 80, 90, 100, 110, 120, 130, 140 keV, DECT-FF (mg/ml)	GE Discovery CT750 HD 1.5 T Signa HDxt Acuson S2000 US (Siemens)
Comparative Study of Ultrasonography, Computed Tomography, Magnetic Resonance Imaging, and Magnetic Resonance Spectroscopy for the Diagnosis of Fatty Liver in a Rat Model	Noh H et al.	2017	Randomized controlled trial	15 (fatty diet), 5 controls	Rats	Histology (< 5 %, 5–33 %, 33–66 %, > 66 %), triglyceride content in biopsy, SECT-HU and difference liver to spleen HU (native, 120 kV, 100 mAs, collimation 0.6 mm, pitch 0.55 mm), MRI-FF (TR 8.83 ms, TE 1.23 ms, 6 echoes, FA 4 °), MRS (TR 3000 ms, TE 12 ms, 5 echo times), ultrasound (echogenicity of liver, spleen)	Native, 80 kV/100 mAs, 140 kV/425 mAS, slice thickness 1.5 mm, collimation 0.6 mm, pitch 0.55, HU at 40 kV and 80 kV, DECT-ΔHU between 40 and 80 keV (liver and spleen separately)	Somatom Definition FLASH (Siemens) Philips iU22 Ultrasound (Philips) 3 T Magnetom Skyra (Siemens)
Multimaterial Decomposition Algorithm for the Quantification of Liver Fat Content by Using Fast-Kilovolt-Peak Switching Dual-Energy CT: Clinical Evaluation	Hyodo T et al.	2017	Prospective cohort study	33 (including 4 without steatosis)	Patients with suspected non-alcoholic fatty liver based on laboratory parameters and ultrasound	Histology (< 5 %, 5–33 %, 33–66 %, > 66 %), MRS (single-shot, TE 28 ms)	Native and contrast-enhanced (arterial, portal-venous, late phase), 80/140 kV, 640 mA, slice thickness 5 mm, HU on virtual monoenergetic images at 70 keV, DECT-FF (%)	GE Discovery CT750 HD 1.5 T Signa HDxt
Evaluation on Heterogeneity of Fatty Liver in Rats: A Multiparameter Quantitative Analysis by Dual-Energy CT	Cao Q et al.	2018	Randomized controlled trial	16 (fatty diet for 8, 12, 16 and 20 weeks, each group 3–4 animals), 8 controls	Rats	Histology (< 5 %, 5–33 %, 33–66 %, > 66 %)	Native, 80/140 kV, slice thickness 2.5 mm, distance 2.5 mm, HU values on virtual monoenergetic images at 40–140 keV in increments of 5 keV, liver to spleen HU difference and quotient at 70 keV, HU curves from 40 to 140 keV, DECT-FF (mg/ml)	GE Discovery CT750 HD

The type of dual-energy computed tomography (DECT) image generation (sequential scanning, fast-kVp-switching computed tomography, or dual-source computed tomography) is specified at first mentioning of the respective scanner type.
SECT = single-energy computed tomography (CT), MRT-FF = magnetic resonance tomography fat fraction, IDEAL = iterative decomposition of water and fat with echo asymmetry and least squares estimation, DECT-FF = DECT-fat fraction, MRS = magnetic resonance spectroscopy.

▶ **Table 2** Overview of included studies concerning fat quantification in bone marrow.

Title	Author	Year	Study design	Number	Study object	Modality of comparison	DECT parameters	Scanner type
A phase I feasibility study of multi-modality imaging assessing rapid expansion of marrow fat and decreased bone mineral density in cancer patients	Hui SK et al.	2015	Cadaver study, controlled cohort study	5 phantoms, 17 cadaver vertebrae, 31 patients, 12 controls	Phantoms (0 %, 50 %, 70 %, 95 % and 100 % fat), lumbar cadaver vertebrae, patients with ovarian and endometrial cancer and scheduled ovariectomy + chemotherapy and with (cohort group) or without (control) adjuvant radiation	Known phantom concentrations, histology of the cadaver vertebrae (adipocyte volume per tissue volume), SECT after 0, 6, 12 months (no information on contrast medium provided, 80 kV in phantoms, 140 kV in patients, QCT Pro software for bone mineral density), MRI-FF in 16 patients after 0, 6, 12 months (TE 2, 3, 4 ms, TR 9 ms), DXA after 0 and 12 months	No information provided on the use of contrast agent, 80 kV, 140 kV, slice thickness 1 mm, DECT bone mineral (mg/cm^3), DECT-FF of the bone marrow (%)	SOMATOM Definition Flash (Dual-Source, Siemens) 3 T TRIO (Siemens) DXA (General Electric)
Marrow Adipose Tissue Quantification of the Lumbar Spine by Using Dual-Energy CT and Single-Voxel (1)H MR Spectroscopy: A Feasibility Study	Bredella MA et al.	2015	Prospective cohort study	12	Overweight and osteopenia patients	MRS (3000/30, 8 acquisitions), SECT bone mineral density	No information provided on the use of contrast agent, 80 kV/210 mAs, 140 kV/80 mAs, slice thickness 2 mm, increment 2 mm, collimation 0.6 mm, pitch 0.9:1, DECT-FF of the bone marrow (%), influence of fatty marrow on bone mineral density determination	SOMATOM Definition Flash 3 T TRIO
Validation of marrow fat assessment using noninvasive imaging with histologic examination of human bone samples	Arentsen L et al.	2015	Cadaver study	20 in MRI and CT, including 17 histological controls	Lumbar cadaver vertebrae	Histology (adipocyte volume per tissue volume), MRI-FF (TE = 2, 3, 4 ms, TR = 9 ms, FA = 1°)	No information provided on the use of contrast agent, 80 kV/140 kV, slice thickness 1 mm, DECT-FF/ DECT volume fraction of the yellow marrow (%)	SOMATOM Definition Flash 3 T TRIO
Evaluation of functional marrow irradiation based on skeletal marrow composition obtained using dual-energy computed tomography,	Magome T et al.	2016	Cadaver study, cohort study	7 cadavers, 6 patients	Cadaver, leukemia patients	Histology in cadavers (fat volume per tissue volume), no control in the patient study	Cadaver study: 80 and 140 kV, patients: 90 and 140 kV, slice thickness 5 mm, collimation 0.98–1.37 mm, calibration of both CT scanners with QCT phantom (Mindways Software, Austin, r = 0.998, p < 0.0001), DECT percentage of red bone marrow (%), DECT-FF (%)	SOMATOM Definition Flash (Siemens) cadaver study, Brilliance Big Bore (Philips) patient study

▲ **Table 2** (Continuation)

Title	Author	Year	Study design	Number	Study object	Modality of comparison	DECT parameters	Scanner type
Use of dual-energy computed tomography to measure skeletal-wide marrow composition and cancellous bone mineral density	Arentsen L et al.	2017	Cadaver study	20	Cadaver	MRI-FF in 20 vertebrae (TE = 2, 3, 4 ms, TR = 9 ms, FA = 1°), bone mineral density (mg/cm³) by micro-CT in 13 vertebrae (1.3-fold magnification, 4-fold binning, 0.5 mm A1 filter, 80 kV)	Native, 80 kV/308 mAs, Sn140 kV/110–150 mAs, DECT bone mineral density (mg/cm³), DECT-FF/content of yellow marrow (%), DECT distribution of red and yellow marrow throughout the body	SOMATOM Definition Flash 3T Trio MRI Inveon Micro CT (Siemens)

The type of dual-energy computed tomography (DECT) image generation (sequential scans, fast-kVp-switching computed tomography, or dual-source computed tomography) is specified at first mentioning of the respective scanner type.
SECT = single-energy computed tomography (CT), DECT-FF = DECT-fat fraction, MRT-FF = magnetic resonance tomography fat fraction, DXA = dual-energy absorptiometry, MRS = magnetic resonance spectroscopy.

ges examined in two studies with fast-kVP-switching DECT in mice and rats ($r = -0.892$ at 40 keV [25], $r^2 \leq 0.88$ at 65 keV [24]). This level of correlation was comparable with the correlation between histology and MRI fat fraction (MRI-FF), which was determined via T2* and DIXON chemical shift relaxometry ($r^2 \leq 0.95$ [24], $r = 0.834$ [27], $r = 0.869$ [28], $r = 0.882$ [25]).

The correlation of the liver to spleen HU difference and quotient with histology was good to moderate in two studies. This applied when using the sequential technique at 140 kV in patients in 1998 and also when using the fast-kVp-switching DECT technique on virtual monoenergetic images at 70 keV in rats in 2018 (difference: $r = 0.75$ at 140 kV [22], $r = -0.844$ to $r = -0.672$ at 70 keV [30], quotient: $r = -0.835$ to $r = -0.657$ at 70 keV [30]). The effective Z-value calculated in two studies in rats and mice correlated on a comparable level with histology ($r = -0.897$ [25] $r = 0.67$ [24]).

If contrast-enhanced examinations are compared to native examinations, the SECT attenuation coefficients on native images correlate very well to well with histology ($r = -0.92$ at 120 kV [23], $r = -0.93$ at 90 kV [23], $r = -0.868$ at 120 kV [27]) but not after contrast agent administration ($p = 0.365$ at 80 kV or 140 kV [27]). The DECT-FF calculated based on material decomposition on native images correlated in the majority of studies well with histology ($r = 0.91$ [25], $r = 0.517$ to $r = 0.816$ [30], [29]). However, in contrast to attenuation coefficients, the DECT-FF both in rabbits and humans ($n = 33$) correlated with the histological grade of steatosis even after contrast agent administration ($r = 0.794$, $p < 0.001$ [27], [29]).

Only the oldest study from 1998 including 5 patients yielded different results compared to the rest of the studies. It did not show a correlation with the histological grade in the iron-free liver for native SECT attenuation coefficients (80, 140 kV) or for the DECT-ΔHU generated using the sequential technique (80, 140 kV) [22]. Another study was able to detect hepatic steatosis (< 5 % versus > 5 % fat) via dual-source DECT even in the case of coexisting iron and fat overload [26].

Value of DECT compared to MRI

Except for one study on dual-source DECT [28], five other studies comparing DECT with MRI used fast-kVp-switching DECT. One of these studies compared DECT with MRI chemical shift relaxometry in patients [5]. Two additional publications examined the agreement between the two modalities in rats [25, 28], one in rabbits [27] and one in mice [24]. The comparison of DECT with MRS was performed in two studies including patients [5, 29] and in two studies with rats [25, 28].

The DECT attenuation coefficients on virtual monoenergetic images acquired with fast-kVp-switching DECT correlated well with the MRI-FF in healthy and leptin-deficient mice ($r^2 = 0.86$ at 65 keV [24]). The level of correlation was thus comparable to that of the native SECT attenuation coefficients compared to MRI-FF ($r^2 = 0.86$) or MRS ($r^2 = 0.86$) in patients [5].

Studies examining the agreement of DECT material decomposition (DECT-FF) results with MRI yielded divergent results. DECT-FF seems to generally agree with MRI-FF in animals ($r^2 \leq 0.67$ in mice [24], $r = 0.652$ in rabbits with a mean difference

▶ **Table 3** Overview of study results on DECT fat quantification.

Target organ	Author	Year	Fat quantification results
Liver	Mendler MH et al.	1998	▪ Correlation of histology with SECT (spleen-liver difference at 140 kV): r = 0.75 ▪ Correlation of histology with DECT-ΔHU (within the liver between 80 and 140 kV) was not significant neither in the iron-free nor in the iron-overloaded liver. ▪ Applying a cut-off of ≥ 12 HU, SECT (spleen-liver difference) detected hepatic steatosis in 2 of 3 cases without coexisting iron and in 2 out of 10 cases with iron overload. ▪ Applying a cut-off of ≥ 9 HU, DECT-ΔHU detected hepatic steatosis in 1 of 5 cases without coexisting iron and in none with iron overload.
	Wang B et al.	2003	▪ Correlation of histology with SECT attenuation coefficients: r = –0.93 (at 90 kV), r = –0.92 (at 120 kV) ▪ Correlation of histology with DECT-ΔHU (between 90 and 120 kV): r = 0.95, p < 0.001
	Artz NS et al.	2012	▪ Correlation of histology with MRI-FF: coefficient of determination $r^2 \leq 0.95$ ▪ Correlation of histology with monoenergetic DECT HU at 65 keV: $r^2 \leq 0.88$; with effective Z: r = 0.67 ▪ Correlation of MRI-FF with monoenergetic DECT HU at 65 keV: $r^2 = 0.85$; with DECT-FF: $r^2 \leq 0.67$ ▪ Correlation of triglyceride mass fraction from biopsies with MRI-FF: $r^2 = 0.92$, p < 0.001; with DECT HU at 65 keV: $r^2 = 0.89$, p < 0.001; with effective Z: $r^2 \leq 0.67$, p < 0.001; and with DECT-FF: $r^2 \leq 0.67$, p < 0.001 ▪ Correlation of phantom fat concentration with MRI-FF: $r^2 = 0.995$, p < 0.001; with DECT HU at 65 keV: $r^2 = 0.999$, p < 0.001; with effective Z: $r^2 = 0.96$, p = 0.003; and with DECT-FF: $r^2 = 0.98$, p = 0.001
	Zheng X et al.	2013	▪ HU values on subtraction maps based on dual-energy data at 75 and 50 keV were significantly larger than those on subtraction maps generated from 140 and 80 keV images (p < 0.001). ▪ Both the liver/spleen quotient and the liver-spleen difference between patients with different grades of steatosis hepatis showed larger differences at a lower keV. Differentiating steatosis grades by the liver/spleen quotient and liver-spleen difference works better at a lower keV.
	Mendonça PRS et al.	2013	The difference between liver fat measured by native SECT and post-contrast DECT-FF was small with a maximum of 3 %. Fat quantification by DECT-FF is feasible even after the application of contrast agent.
	Patel BN al.	2013	▪ Correlation of native SECT (liver-spleen difference for HU values < 1, which were regarded as clinically relevant hepatic steatosis) with post-contrast DECT-FF: r = 0.74, p < 0.001 Fat quantification by DECT-FF is feasible even after the application of contrast agent ▪ AUROC DECT-FF 0.85
	Mendonça PRS et al.	2014	Please see Mendonça PRS et al. 2013
	Sun T et al.	2014	▪ Correlation of histology with DECT-HU at 40 keV: r = –0.892, p < 0.001; with the effective Z: r = –0.897, p < 0.001; and with DECT-FF: r = 0.91, p < 0.001 ▪ Correlation of histology with MRI-FF: r = 0.882, p < 0.001; and with MRS: r = 0.894, p < 0.001 ▪ AUROC MRT-FF 0.97; AUROC MRS 0.98 ▪ AUROC DECT-FF 0.95
	Ma J et al.	2014	▪ Detection of steatosis hepatis (< 5 % versus > 5 % fat) by iron-specific DECT material decomposition is feasible in patients with coexisting fat and iron overload ▪ Correlation of histology with virtual monoenergetic DECT HU in the iron-free liver: r = –0.642, p < 0.001 ▪ Virtual monoenergetic DECT HU differs significantly between healthy and fatty liver (p = 0.035)

▶ **Table 3** (Continuation)

Target organ	Author	Year	Fat quantification results
	Hur BY et al.	2014	▪ Correlation of histology with native SECT HU: r = –0.868, p < 0.001; and with MRI-FF: r = 0.834 ▪ No significant correlation was found between histology and SECT HU after the application of contrast agent (p = 0.365) ▪ Correlation of histology with DECT-FF existed even after the application of contrast agent: r = 0.79, p < 0.001 ▪ Correlation of MRI-FF with DECT-FF after the application of contrast agent: r = 0.652, p = 0.008 ▪ Mean difference between MRI-FF and DECT-FF after the application of contrast agent: 1.56 % ▪ AUROC native SECT-HU 0.96 (≥ 5 % steatosis) ▪ AUROC MRI-FF 0.89 ▪ AUROC DECT-FF after the application of contrast agent 0.92 (≥ 5 % steatosis)
	Kramer H et al.	2017	▪ Correlation of native SECT HU with MRI-FF and MRS was good: coefficient of determination r^2 = 0.86 (MRI-FF), r^2 = 0.86 (MRS), except for MRS at steatosis grade 0 (< 5.56 % fat: r^2 = 0.07 anterior liver segments, r^2 = 0.01 posterior liver segments) ▪ Correlation of DECT-FF with MRS: r^2 = 0.423 anterior liver segments, r^2 = 0.257 posterior liver segments
	Noh H et al.	2017	▪ Correlation of histology with SECT: r = –0.867; with MRI-FF: r = 0.869; with MRS: r = 0.916; and with DECT-ΔHU: r = 0.775 ▪ AUROC MRT-FF 0.93; AUROC MRS 0.96 ▪ AUROC native SECT (liver-spleen difference) 0.96 ▪ AUROC native DECT-ΔHU 0.95
	Hyodo T et al.	2017	▪ Histology correlates with both native DECT-FF and DECT-FF after the application of contrast agent ▪ The mean difference between native monoenergetic DECT-HU at 70 keV and DECT-FF in the arterial and the portal-venous phase was 10–20 %. ▪ Maximal difference between DECT-FF in native, arterial, portal-venous and late phases was 2 % (p < 0.05) ▪ AUROC MRS 0.89 ▪ AUROC DECT-FF 0.88
	Cao Q et al.	2018	▪ Correlation of histology with DECT-HU at 70 keV (liver/spleen DECT HU): r = –0.835 left lobe, r = –0.657 right lobe. ▪ Correlation of histology with DECT-HU at 70 keV (liver-spleen difference DECT HU): r = –0.844 left lobe, r = –0.672 right lobe. ▪ Correlation of histology with DECT-FF: r = 0.816 left lobe, r = 0.517 right lobe.
Bone marrow	Hui SK et al.	2015	▪ Correlation of histology with DECT-FF in cadavers: r = 0.8 ▪ Correlation of histology with MRI-FF in cadavers: r = 0.77 ▪ Correlation of DECT-FF with MRI-FF in patients: overall r = 0.77 (baseline r = 0.8, after 6 months r = 0.68, after 12 months r = 0.66) ▪ Bone marrow fat increased under therapy (p < 0.002, correlation of bone marrow increase measured by DECT-FF and MRI-FF: r = 0.91) ▪ Negative correlation of bone marrow fat (DECT-FF) and bone mineral density measured by DECT material decomposition at baseline was no longer present 12 months after therapy (baseline: r = –0.8, after therapy: r = –0.26) Increase of bone marrow fat was not accompanied by a decrease of bone mineral density ▪ Coefficient of variation between three different slices within one vertebral body in histology was 0.08
	Bredella MA et al.	2015	▪ Correlation of DECT-FF with MRS: r = 0.91, p < 0.001 ▪ Mean difference between DECT-FF and MRS: –0.02 %, SD ± 1.96 ▪ The averaged not corrected bone mineral density (qSECT) was 124.9 mg/cm3 ± 31.7 ▪ Corrected by the bone marrow fat (DECT-FF) the average bone mineral density was 160.8 mg/cm3 ± 20.7 The mean difference between uncorrected and corrected bone mineral density was –35.9 mg/cm3 (95 % CI –83.4, 11.5) The correlation of the difference between uncorrected and corrected bone mineral density with DECT-FF was excellent (r = 0.99, p < 0.001). The correlation with MRS-FF was good (r = 0.87, p < 0.01)

▲ **Table 3** (Continuation)

Target organ	Author	Year	Fat quantification results
	Arentsen L et al.	2015	▪ Correlation of histology with DECT-FF: r = 0.8 and MRT-FF: r = 0.77 ▪ Correlation between DECT-FF and MRT-FF: r = 0.88 ▪ Coefficient of variation between three different slices within one vertebral body in histology: 0.08
	Magome T et al.	2016	▪ Correlation between histology and DECT-FF: r = 0.86, p < 0.0001
	Arentsen L et al.	2017	▪ Correlation of DECT-FF and MRT-FF: r = 0.88 ▪ qSECT significantly overestimated bone mineral density in the cervical and thoracic spine ▪ qSECT values for peripheral bones with high amounts of yellow bone marrow, e. g. the tibia, were lower than DECT values Differences between uncorrected bone mineral density (qSECT) and bone mineral density corrected by bone marrow fat (DECT) were significant in 14 of 23 skeletal regions (p < 0.05) and even within some individual bones, e. g. femur (between 40 and 62 mg/cm3, p < 0.001)

Study results on fat quantification by dual-energy computed tomography (DECT) and its modalities of comparison are displayed separately for target organs.
SECT = single-energy computed tomography, DECT-FF = DECT fat fraction, MRI-FF = chemical shift relaxometry fat fraction, MRS = magnetic resonance spectroscopy, AUROC = area under the ROC curve, qSECT = quantitative SECT for determination of bone mineral density.

according to Bland-Altman of 1.56 % [27]). However, the correlation between DECT-FF and MRS in humans was described in one study as limited (r^2 = 0.423 liver segments V/VIII, r^2 = 0.257 liver segments VI/VII, n = 50 [5]). Another study showed good diagnostic accuracy for DECT-FF (0.88 area under the ROC curve [29]).

All studies in humans and animals determining the diagnostic accuracy of DECT analyses compared to MRI showed a comparable level. Therefore, an area under the ROC curve (AUROC) of 0.95 was specified for DECT-ΔHU in rats (80, 140 keV [28]). The AUROC was 0.95 for DECT-FF in rats [25], 0.92 on contrast-enhanced scans of rabbits [27], and 0.88 on native scans of patients [29]. These values were similar to the data regarding the diagnostic accuracy of MRI with an AUROC for MRI-FF of 0.97 and 0.93 in rats [25, 28], 0.89 for MRI-FF in rabbits [27], 0.98 and 0.96 for MRS in rats [25, 28] and 0.89 for MRS in humans [29].

Value of DECT compared to SECT

In nine studies DECT fat quantification and SECT fat quantification in the liver were compared. With respect to SECT, all analyses of attenuation coefficients are performed using non-virtual datasets. In five studies, native as well as contrast-enhanced examinations were performed [22, 27, 32–34]. It must be taken into consideration that two of these publications have different method descriptions and different aspects of an identical study protocol with respect to results [32, 33]. SECT tube voltages between 100 and 140 kV were used (see ▶ **Table 1** for CT parameters). Four studies were conducted in humans [5, 22, 31–34], one in mice [24], one in rats [28], and one in rabbits [27].

On native SECT images, the attenuation coefficients in mice correlated well with the attenuation coefficients on virtual monoenergetic images generated by fast-kVp-switching DECT (r^2 = 0.88 for 65 keV [24]). The detection of hepatic steatosis by attenuation coefficients was possible in rats at a setting of up to ≤ 120 k(e)V [28]. Starting at 140 kV, it was no longer possible to differentiate between healthy liver and grade I hepatic steatosis on the basis of attenuation coefficients [28]. However, this was still possible using ΔDECT-HU (p = 0.004, 80 and 140 kV [28]). The differentiation between various grades of steatosis in humans based on the liver to spleen HU difference and quotient was also better at a lower keV setting [31]. The HU values on subtraction images at 75 and 50 keV were also significantly higher than those of subtraction images at 140 and 80 keV (p < 0.001 [31]).

DECT continues to be advantageous in contrast-enhanced examinations. Therefore, the histological grades of steatosis in one study with rabbits could only be differentiated in native SECT (p < 0.001 [27]) but not after contrast agent administration (p = 0.365 [27]). For DECT-FF good correlation with the (histological) grades of steatosis was described also after contrast agent administration (r = 0.79 [27]). Also in humans DECT-FF in contrast-enhanced examinations correlated well with native SECT attenuation coefficients in clinically relevant hepatic steatosis (r = 0.74 [34]) with a maximum difference of 3 % [32]. Compared to DECT HU at 70 keV, the DECT-FF in one study using MRS as a comparison modality was independent of the contrast phase [29]. The maximum difference between the native, arterial, portal-venous, and late phases was 2 % (p < 0.05 [29]).

The diagnostic accuracy between DECT analyses and native SECT is comparable to the previously described diagnostic accuracy between DECT analyses and MRI. Therefore, an AUROC of 0.95 is specified for DECT-ΔHU in rats (native, 80, 140 kV [28]) and an AUROC of 0.92 for DECT-FF in rabbits after contrast agent administration (≥ 5 % steatosis [27]) compared to an AUROC for SECT of 0.96 in rats (native liver-spleen difference, 120 kV [28]) and 0.96 in rabbits (native hepatic HU, 120 kV, ≥ 5 % steatosis [27]). The AUROC for DECT-FF in humans was slightly lower (0.85) [34].

The results of Mendler et al. were cited multiple times in the included literature. This study found DECT to be inferior to SECT for the diagnosis of steatosis. This is particularly true in the case of concomitant iron overload. Therefore, two of three cases without iron overload and two of ten cases with iron overload were able to be detected in SECT (liver-spleen difference, 140 kV). Only one of five cases without iron overload and none with iron overload could be detected by DECT-ΔHU (80, 140 kV). However, the sequential generation of DECT images and the low number of cases (16: 11 with iron overload and 5 without) should be taken into consideration as a limitation. The lack of analyses of DECT material decomposition (DECT-FF) and the lack of comparison of native and contrast-enhanced examinations also limit the significance of these study results.

Results: Fat quantification in bone marrow

Three of a total of five studies on fat quantification in bone marrow compared DECT results with histological examinations in vertebral bodies in cadavers [36–38]. Three studies compared DECT with MRI-FF [36, 37, 39] and one with MRS [40]. In two studies DECT was also used to correct the influence of bone marrow fat on the determination of bone mineral density in quantitative SECT (qSECT) [39, 40]. All studies were performed with dual-source DECT (see ▶ **Table 2** for details regarding study method). An overview of the results of each study is shown in ▶ **Table 3**.

Value of DECT compared to histology

The three studies with partial histological correlations used vertebral bodies from human cadavers. The fat content in bone marrow was histologically determined as the adipocyte volume per tissue volume of the middle layer of the lumbar vertebral body in cadavers. The deviations between this layer and the layers 0.5 cm above and below were minimal in two studies (coefficient of variation 0.08 [36, 37]).

The correlation of DECT-FF in bone marrow with the histological result was good to very good in all three studies (r = 0.8 [37], r = 0.861 [38], r = 0.80 [36]). It was thus slightly superior to the level of correlation between MRI-FF and histology (r = 0.77 [37], r = 0.77 [36]).

Value of DECT compared to MRI

The correlation of DECT-FF in bone marrow with MRS was determined in only one study (high in n = 12 patients, r = 0.91 [40]). The average difference between DECT material decomposition and the fat percentage determined by MRS was –0.02 % (SD ± 1.96) in this cohort [40].

The correlation between the DECT-FF and the MRI-FF was slightly lower (r = 0.77 [36], 0.88 [37] [39]) in one study including patients with ovarian/endometrial cancer (n = 31) and in two studies using cadaver vertebral bodies. However, this level of correlation was maintained over the course of treatment, after ovariectomy, chemotherapy and/or radiation, with a 7–15 % increase in vertebral body fat (r = 0.91 [36]).

Interestingly, the negative correlation of the bone marrow fat percentage determined in the initial examination with the bone mineral density determined by DECT material decomposition could no longer be detected 12 months after treatment (baseline: r = –0.8 DECT-FF, r = –0.79 MRI-FF; after treatment: r = –0.26 DECT-FF, r = 0.051 MRI-FF [36]). The increase in vertebral body fat during treatment was thus not associated with an automatic decrease in bone mineral density.

Value of DECT compared to SECT

The effect of the bone marrow fat content determined by DECT material decomposition (DECT-FF) on the bone mineral percentage calculated in qSECT at 140 kV was examined in two studies.

If the bone mineral density determined by qSECT was corrected by the fat percentage in bone marrow determined by DECT-FF, there was a difference between the corrected and uncorrected bone mineral density of –35.9 mg/cm^3 (–27.2 %, CI –83.4, 11.5 [40]) in the cohort of osteopenic, overweight patients (n = 12). The difference correlated with the bone marrow fat percentage in the MRI-FF (r = 0.87 [40]). An increase in the bone marrow fat percentage resulted in a corresponding increase in the measurement error for bone mineral density in SECT.

In relation to the various skeletal regions, the difference between corrected and uncorrected bone mineral density was significant (p < 0,05 [39]) in 14 of 23 skeletal regions in human cadavers (n = 20). Particularly for skeletal regions with significant yellow bone marrow, e. g. tibia and humerus, the correlation of the amount of bone marrow fat (DECT-FF) with the difference between corrected and uncorrected bone mineral density was high (r = 0.93, p < 0.0001 [39]). In some cases, significant differences between corrected and uncorrected bone mineral density within a single bone could be identified by correcting the bone mineral density by the DECT-FF bone marrow fat percentage (p < 0.001 [39]).

Discussion

The heterogeneity of the included studies on DECT fat quantification was high with respect to hardware (sequential generation of DECT data, fast-kVP-switching DECT, dual-source DECT), DECT analysis methods (including attenuation coefficients on virtual monoenergetic images, DECT-ΔHU, DECT-FF), and test subjects (small animals, patients). All studies were related to the liver and bone marrow. However, there were fewer studies on bone marrow.

Based on the included studies, fat quantification via DECT analyses yields valid results in the animal model and in patients compared to histology, SECT and MRI for the liver and bone marrow.

Hepatic steatosis

According to the currently available studies, hepatic steatosis and its grade can be reliably diagnosed by DECT. One advantage of DECT compared to SECT is the possibility to generate virtual monoenergetic images at a lower keV setting. These images were more sensitive for the diagnosis of hepatic steatosis due to the higher soft-tissue contrast. Moreover, DECT material decomposition provides quantitative fat data compared to semiquantitative attenuation coefficients [32]. DECT is clearly superior to SECT according to the currently available studies primarily in contrast-enhanced CT examinations which make up the majority of clinically indicated abdominal CT examinations. Therefore, DECT material decomposition allows valid determination of the fat percentage regardless of the contrast phase. Moreover, the suitability of DECT even after contrast agent administration and the various possible approaches to DECT fat quantification put the study result of Mender et al. into perspective. In this study which found DECT to be extremely limited or unsuitable for fat quantification in the liver only the difference in attenuation coefficients between 80 kV und 140 kV in sequential native DECT in a small collective was examined.

Both MRI chemical shift relaxometry and MRS are suitable as noninvasive control techniques for DECT studies as demonstrated by the good correlation to histological degrees of steatosis. One limitation is that only small organ segments are examined by MRS and in histology. Techniques like MRI relaxometry, SECT, and DECT must thus always be used to diagnose irregular fatty lesions.

Bone marrow fat

The use of DECT material decomposition proved to be advantageous for determining fat content in bone marrow, particularly for the correction of the bone mineral percentage. A bone mineral density measurement error that increases with an increasing fat content as in qSECT could be corrected by DECT. This is also an advantage compared to dual-energy X-ray absorptiometry (DXA), which as a widely available method for bone mineral measurement is subject to comparable limitations [3]. Prospectively, additional DXA or qSECT examinations for detecting osteoporosis in patients who already underwent a DECT examination for another indication could be avoided to reduce radiation.

The MRI-FF and particularly also MRS as noninvasive control techniques are also suitable for studies on DECT fat quantification in bone marrow.

Regardless of the suitability of DECT for fat quantification in the liver and bone marrow, the inherent advantages and disadvantages of the various modalities must be taken into consideration. Therefore, the short examination times and the higher compatibility in (DE)CT compared to MRI are advantageous in patients with foreign material or claustrophobia. However, due to the inherent radiation exposure, DECT liver fat quantification can only be performed given an existing clinical indication for CT. Particularly when contrast agent administration is planned, DECT would be preferable to SECT.

Due to the potentially false bone mineral density values at a high bone marrow fat percentage in DXA [3] and qSECT [39, 40], the use of DECT as an alternative to qSECT should be examined. Additional studies comparing the radiation exposure of the two modalities for determining bone mineral density, e. g. in cadavers, are needed for this purpose. Compared to histology, all imaging modalities avoid intervention-based side effects like bleeding, nerve and organ injury, and infections.

Limitations

It cannot be ruled out that some studies were not included based on the selected search parameters (see ▶ **Fig. 2**). Due to the necessary addition of "not iodine" to rule out studies on iodine quantification, studies, in which both iodine and fat had been quantified would not have been selected. Due to the focus of all included studies on the liver and bone marrow, no statements regarding the validity of DECT fat quantification in other organ systems can be made. However, one study from the literature search that was not included due to the lack of comparison modalities for validating DECT results shows the benefit of DECT fat measurements for differentiating benign from malignant adrenal masses [4]. The focus of the included studies on the liver and bone marrow could be based on the clinical relevance of the diagnosis of hepatic steatosis and the measurement of the fat percentage in bone marrow. The prevalence of nonalcoholic fatty liver disease (NALFD) ranges from 13.5 % (Africa) to 46 % (USA) with an increasing tendency [41]. Fatty changes of bone marrow are an age-independent process that occurs to varying degrees and is associated with diseases like leukemia and corresponding treatments [36]. Depending on the fat percentage in bone marrow, there is a high measurement error in conventional methods for bone mineral measurement [39, 40]. Therefore, valid individual determination of the percentage of fatty bone marrow is highly relevant.

Patients with coexisting hepatic fat and iron overload represent clinically relevant special cases. There are numerous studies examining the effect of fat on DECT iron measurements in the liver [42–46]. However, these were excluded since their focus was on iron measurement and not fat measurement or because no in vivo validation on the basis of comparison modalities was performed for the fat measurements. Consequently, it is only possible to state that the differentiation of healthy liver from steatotic liver even in the case of iron overload seems possible [26].

Apart from the already indicated study heterogeneity, some studies lacked data regarding the relevant measurement parameters. In some cases it was only stated that standard abdominal protocols were used. It was not specified whether contrast agent was used [31]. In some cases, information regarding the tube voltage, tube current [32–34] or the general CT and MRI parameters [32, 33] was not provided.

Moreover, the lack of studies examining fat content via dual-layer spectral CT or split-filter DECT is noteworthy. This may be due to the fact that these techniques were only recently intro-

duced in clinical centers. Studies on DECT fat quantification by dual-layer spectral CT or split-filter DECT would thus be desirable.

There is also potential for complementary studies to validate DECT fat quantification on the basis of comparison modalities in other organ systems. For example, more reliable in vitro differentiation of fat and arterial and venous thrombi as seen in vascular plaque was described for DECT compared to SECT [19]. The suitability of DECT for differentiating between plaque with high fat percentages and low fat percentages in vessels in vivo should be examined accordingly. The fat percentage in skeletal muscle, which has been determined to date based on morphological imaging data or semiquantitatively via SECT attenuation coefficients [47], could also be quantified via DECT.

Conclusion

DECT is a valid technique for fat quantification in the liver and bone marrow. In contrast to SECT, DECT can be used for reliable diagnosis of hepatic steatosis and its extent not only in native but also in contrast-enhanced CT examinations. In bone, DECT measurement of the bone marrow fat percentage allows more exact determination of the bone mineral density than conventional methods. Given the heterogeneity of the studies as well as the lack of studies on other organ systems, dual-layer spectral CT, and split-filter DECT, there is a need for additional studies on DECT fat quantification.

Conflict of Interest

The authors declare that they have no conflict of interest.

References

[1] Anstee QM, Reeves HL, Kotsiliti E et al. From NASH to HCC: current concepts and future challenges. Nat Rev Gastroenterol Hepatol 2019; 16: 411–428. doi:10.1038/s41575-019-0145-7

[2] Wehrli FW, Hopkins JA, Hwang SN et al. Cross-sectional study of osteopenia with quantitative MR imaging and bone densitometry. Radiology 2000; 217: 527–538. doi:10.1148/radiology.217.2.r00nv20527

[3] Bolotin HH. DXA in vivo BMD methodology: an erroneous and misleading research and clinical gauge of bone mineral status, bone fragility, and bone remodelling. Bone 2007; 41: 138–154. doi:10.1016/j.bone.2007.02.022

[4] Ju Y, Liu A, Dong Y et al. The Value of Nonenhanced Single-Source Dual-Energy CT for Differentiating Metastases From Adenoma in Adrenal Glands. Academic radiology 2015; 22: 834–839. doi:10.1016/j.acra.2015.03.004

[5] Kramer H, Pickhardt PJ, Kliewer MA et al. Accuracy of Liver Fat Quantification With Advanced CT, MRI, and Ultrasound Techniques: Prospective Comparison With MR Spectroscopy. Am J Roentgenol American journal of roentgenology 2017; 208: 92–100. doi:10.2214/ajr.16.16565

[6] Ferraioli G, Soares Monteiro LB. Ultrasound-based techniques for the diagnosis of liver steatosis. World J Gastroenterol 2019; 25: 6053–6062. doi:10.3748/wjg.v25.i40.6053

[7] Li Q, Dhyani M, Grajo JR et al. Current status of imaging in nonalcoholic fatty liver disease. World J Hepatol 2018; 10: 530–542. doi:10.4254/wjh.v10.i8.530

[8] Hounsfield GN. Computerized transverse axial scanning (tomography). 1. Description of system. The British journal of radiology 1973; 46: 1016–1022. doi:10.1259/0007-1285-46-552-1016

[9] Marshall WH Jr, Easter W, Zatz LM. Analysis of the dense lesion at computed tomography with dual kVp scans. Radiology 1977; 124: 87–89. doi:10.1148/124.1.87

[10] Johnson TR, Krauss B, Sedlmair M et al. Material differentiation by dual energy CT: initial experience. European radiology 2007; 17: 1510–1517. doi:10.1007/s00330-006-0517-6

[11] Johnson TR. Dual-energy CT: general principles. Am J Roentgenol American journal of roentgenology 2012; 199: S3–S8

[12] Flohr TG, McCollough CH, Bruder H et al. First performance evaluation of a dual-source CT (DSCT) system. European radiology 2006; 16: 256–268. doi:10.1007/s00330-005-2919-2

[13] Rutt B, Fenster A. Split-filter computed tomography: a simple technique for dual energy scanning. Journal of computer assisted tomography 1980; 4: 501–509. doi:10.1097/00004728-198008000-00019

[14] Euler A, Parakh A, Falkowski AL et al. Initial Results of a Single-Source Dual-Energy Computed Tomography Technique Using a Split-Filter: Assessment of Image Quality, Radiation Dose, and Accuracy of Dual-Energy Applications in an In Vitro and In Vivo Study. Investigative radiology 2016; 51: 491–498. doi:10.1097/RLI.0000000000000257

[15] Rassouli N, Etesami M, Dhanantwari A et al. Detector-based spectral CT with a novel dual-layer technology: principles and applications. Insights Imaging 2017; 8: 589–598. doi:10.1007/s13244-017-0571-4

[16] Zhang YN, Fowler KJ, Hamilton G et al. Liver fat imaging-a clinical overview of ultrasound, CT, and MR imaging. The British journal of radiology 2018; 91: 20170959. doi:10.1259/bjr.20170959

[17] Singhal V, Bredella MA. Marrow adipose tissue imaging in humans. Bone 2019; 118: 69–76. doi:10.1016/j.bone.2018.01.009

[18] Yang CB, Zhang S, Jia YJ et al. Clinical Application of Dual-Energy Spectral Computed Tomography in Detecting Cholesterol Gallstones From Surrounding Bile. Academic radiology 2017; 24: 478–482. doi:10.1016/j.acra.2016.10.006

[19] Zachrisson H, Engstrom E, Engvall J et al. Soft tissue discrimination ex vivo by dual energy computed tomography. European journal of radiology 2010; 75: e124–e128. doi:10.1016/j.ejrad.2010.02.001

[20] Ohta Y, Kitao S, Watanabe T et al. Evaluation of image quality of coronary artery plaque with rapid kVp-switching dual-energy CT. Clinical imaging 2017; 43: 42–49. doi:10.1016/j.clinimag.2017.01.014

[21] Tang CX, Zhou CS, Zhao YE et al. Detection of pulmonary fat embolism with dual-energy CT: an experimental study in rabbits. European radiology 2017; 27: 1377–1385. doi:10.1007/s00330-016-4512-2

[22] Mendler MH, Bouillet P, Le Sidaner A et al. Dual-energy CT in the diagnosis and quantification of fatty liver: limited clinical value in comparison to ultrasound scan and single-energy CT, with special reference to iron overload. J Hepatol 1998; 28: 785–794. doi:10.1016/s0168-8278(98)80228-6

[23] Wang B, Gao Z, Zou Q et al. Quantitative diagnosis of fatty liver with dual-energy CT. An experimental study in rabbits. Acta radiologica (Stockholm, Sweden : 1987) 2003; 44: 92–97

[24] Artz NS, Hines CD, Brunner ST et al. Quantification of hepatic steatosis with dual-energy computed tomography: comparison with tissue reference standards and quantitative magnetic resonance imaging in the ob/ob mouse. Investigative radiology 2012; 47: 603–610. doi:10.1097/RLI.0b013e318261fad0

[25] Sun T, Lin X, Chen K. Evaluation of hepatic steatosis using dual-energy CT with MR comparison. Frontiers in bioscience (Landmark edition) 2014; 19: 1377–1385

[26] Ma J, Song ZQ, Yan FH. Separation of hepatic iron and fat by dual-source dual-energy computed tomography based on material decomposition: an animal study. PLoS One 2014; 9: e110964. doi:10.1371/journal.pone.0110964

[27] Hur BY, Lee JM, Hyunsik W et al. Quantification of the fat fraction in the liver using dual-energy computed tomography and multimaterial decomposition. Journal of computer assisted tomography 2014; 38: 845–852. doi:10.1097/RCT.0000000000000142

[28] Noh H, Song X, Heo SH et al. Comparative Study of Ultrasonography, Computed Tomography, Magnetic Resonance Imaging, and Magnetic Resonance Spectroscopy for the Diagnosis of Fatty Liver in a Rat Model. J Korean Soc Radiol 2017; 76: 14–24

[29] Hyodo T, Yada N, Hori M et al. Multimaterial Decomposition Algorithm for the Quantification of Liver Fat Content by Using Fast-Kilovolt-Peak Switching Dual-Energy CT: Clinical Evaluation. Radiology 2017; 283: 108–118. doi:10.1148/radiol.2017160130

[30] Cao Q, Shang S, Han X et al. Evaluation on Heterogeneity of Fatty Liver in Rats: A Multiparameter Quantitative Analysis by Dual Energy CT. Academic radiology 2019; 26: e47–e55. doi:10.1016/j.acra.2018.05.013

[31] Zheng X, Ren Y, Philips WT et al. Assessment of hepatic fatty infiltration using spectral computed tomography imaging: a pilot study. J Comput Assist Tomogr 2013; 37: 134–141

[32] Mendonca PR, Lamb P, Kriston A et al. Contrast-independent liver-fat quantification from spectral CT exams. Med Image Comput Comput Assist Interv 2013; 16: 324–331

[33] Mendonca PR, Lamb P, Sahani DV. A Flexible Method for Multi-Material Decomposition of Dual-Energy CT Images. IEEE transactions on medical imaging 2014; 33: 99–116. doi:10.1109/tmi.2013.2281719

[34] Patel BN, Kumbla RA, Berland LL et al. Material density hepatic steatosis quantification on intravenous contrast-enhanced rapid kilovolt (peak)-switching single-source dual-energy computed tomography. Journal of computer assisted tomography 2013; 37: 904–910. doi:10.1097/RCT.0000000000000027

[35] Brunt EM, Janney CG, Di Bisceglie AM et al. Nonalcoholic steatohepatitis: a proposal for grading and staging the histological lesions. Am J Gastroenterol 1999; 94: 2467–2474. doi:10.1111/j.1572-0241.1999.01377.x

[36] Hui SK, Arentsen L, Sueblinvong T et al. A phase I feasibility study of multi-modality imaging assessing rapid expansion of marrow fat and decreased bone mineral density in cancer patients. Bone 2015; 73: 90–97. doi:10.1016/j.bone.2014.12.014

[37] Arentsen L, Yagi M, Takahashi Y et al. Validation of marrow fat assessment using noninvasive imaging with histologic examination of human bone samples. Bone 2015; 72: 118–122. doi:10.1016/j.bone.2014.11.002

[38] Magome T, Froelich J, Takahashi Y et al. Evaluation of Functional Marrow Irradiation Based on Skeletal Marrow Composition Obtained Using Dual-Energy Computed Tomography. Int J Radiat Oncol Biol Phys 2016; 96: 679–687. doi:10.1016/j.ijrobp.2016.06.2459

[39] Arentsen L, Hansen KE, Yagi M et al. Use of dual-energy computed tomography to measure skeletal-wide marrow composition and cancellous bone mineral density. J Bone Miner Metab 2017; 35: 428–436

[40] Bredella MA, Daley SM, Kalra MK et al. Marrow Adipose Tissue Quantification of the Lumbar Spine by Using Dual-Energy CT and Single-Voxel (1)H MR Spectroscopy: A Feasibility Study. Radiology 2015; 277: 230–235. doi:10.1148/radiol.2015142876

[41] Perumpail BJ, Khan MA, Yoo ER et al. Clinical epidemiology and disease burden of nonalcoholic fatty liver disease. World J Gastroenterol 2017; 23: 8263–8276. doi:10.3748/wjg.v23.i47.8263

[42] Hyodo T, Hori M, Lamb P et al. Multimaterial Decomposition Algorithm for the Quantification of Liver Fat Content by Using Fast-Kilovolt-Peak Switching Dual-Energy CT: Experimental Validation. Radiology 2017; 282: 381–389. doi:10.1148/radiol.2016160129

[43] Fischer MA, Gnannt R, Raptis D et al. Quantification of liver fat in the presence of iron and iodine: an ex-vivo dual-energy CT study. Investigative radiology 2011; 46: 351–358. doi:10.1097/RLI.0b013e31820e1486

[44] Xie T, Li Y, He G et al. The influence of liver fat deposition on the quantification of the liver-iron fraction using fast-kilovolt-peak switching dual-energy CT imaging and material decomposition technique: an in vitro experimental study. Quantitative imaging in medicine and surgery 2019; 9: 654–661. doi:10.21037/qims.2019.04.06

[45] Fischer MA, Reiner CS, Raptis D et al. Quantification of liver iron content with CT-added value of dual-energy. European radiology 2011; 21: 1727–1732. doi:10.1007/s00330-011-2119-1

[46] Oelckers S, Graeff W. In situ measurement of iron overload in liver tissue by dual-energy methods. Physics in medicine and biology 1996; 41: 1149–1165. doi:10.1088/0031-9155/41/7/006

[47] Poltronieri TS, de Paula NS, Chaves GV. Assessing skeletal muscle radiodensity by computed tomography: An integrative review of the applied methodologies. Clin Physiol Funct Imaging 2020. doi:10.1111/cpf.12629

[48] Cruz-Jentoft AJ, Bahat G, Bauer J et al. Sarcopenia: revised European consensus on definition and diagnosis. Age Ageing 2019; 48: 16–31. doi:10.1093/ageing/afy169